RAPID COMMUNICATIONS

PHYSICAL REVIEW MATERIALS **1**, 062001(R) (2017)

Two-dimensional electron system at the magnetically tunable EuO/$SrTiO_3$ interface

Patrick Lömker,[1] Tobias C. Rödel,[2,3,4] Timm Gerber,[1] Franck Fortuna,[2] Emmanouil Frantzeskakis,[2] Patrick Le Fèvre,[3] François Bertran,[3] Martina Müller,[1,5,*] and Andrés F. Santander-Syro[2,†]

[1]*Peter Grünberg Institut (PGI-6), Forschungszentrum Jülich GmbH, D-52428 Jülich, Germany*

[2]*CSNSM, Univ. Paris-Sud, CNRS/IN2P3, Université Paris-Saclay, 91405 Orsay Cedex, France*

[3]*Synchrotron SOLEIL, L'Orme des Merisiers, Saint-Aubin-BP48, 91192 Gif-sur-Yvette, France*

[4]*Laboratory for Photovoltaics, Physics and Material Science Research Unit, University of Luxembourg, L-4422 Belvaux, Luxembourg*

[5]*Fakultät Physik, Technische Universität Dortmund, D-44221 Dortmund, Germany*

(Received 23 March 2017; published 14 November 2017)

We create a two-dimensional electron system (2DES) at the interface between EuO, a ferromagnetic insulator, and $SrTiO_3$, a transparent nonmagnetic insulator considered the bedrock of oxide-based electronics. This is achieved by a controlled *in situ* redox reaction between pure metallic Eu deposited at room temperature on the surface of $SrTiO_3$—an innovative bottom-up approach that can be easily generalized to other functional oxides and scaled to applications. Additionally, we find that the resulting EuO capping layer can be tuned from paramagnetic to ferromagnetic, depending on the layer thickness. These results demonstrate that the simple, novel technique of creating 2DESs in oxides by deposition of elementary reducing agents [T. C. Rödel *et al.*, Adv. Mater. **28**, 1976 (2016)] can be extended to simultaneously produce an *active*, e.g., magnetic, capping layer enabling the realization and control of additional functionalities in such oxide-based 2DESs.

DOI: 10.1103/PhysRevMaterials.1.062001

Introduction. Two-dimensional electron systems (2DESs) in functional oxides have gained strong interest as a novel state of matter with fascinating and exotic interface physics. For instance, the 2DES in $LaAlO_3/SrTiO_3$ (LAO/STO) interfaces can host metal-to-insulator transitions, superconductivity and magnetism—all of them tunable by gate electric fields [1–9]. The prospect of creating and manipulating a macroscopic magnetic ground state in oxide-based 2DESs is of enormous interest, as this would pave the route towards oxide spintronic applications with novel quantum phases beyond today's semiconductor technology at the LAO/STO interface, e.g., by the observation of tunnel magnetoresistance (TMR) [10] or the inverse Edelstein effect [11,12]. The magnetic field dependence of TMR was attributed to a Rashba-type spin-orbit coupling, potentially allowing the manipulation of spin polarization in a 2DES, whereas its spin-momentum locking may enable a high efficiency of the conversion of an injected spin current into a charge current. In fact, in the case of the LAO/STO interface, it was recently demonstrated that additional epitaxial ferroic oxide layers can be used to tune the spin polarization of the 2DES by an electric field [13] or to control its conduction in a nonvolatile manner by ferroelectric switching [14]. So far, the design of functional 2DES required a single layer growth control of epitaxial LAO onto $SrTiO_3$. The emergence of interfacial quantum states, such as magnetism, superconductivity, or spin-orbit coupling, only sets in at a critical LAO thickness of 4 unit cells and in certain regions of the 2DES phase diagram [10]. This conundrum was circumvented by the finding that 2DESs could be fabricated at the bare surface of several oxides, through the creation of oxygen vacancies at their surface [15–22]. These surface 2DESs can also show magnetic domains [23], thus constituting an appealing alternative for the use and control of electric and magnetic properties of confined states in oxides.

Here, we show that insulating and ferromagnetic EuO can be grown on $SrTiO_3$ while simultaneously creating a 2DES at the interface. As schematized in Fig. 1, the fabrication of the 2DES is simply accomplished by the deposition of pure metallic Eu at room temperature in ultrahigh vacuum. We find that the resulting EuO capping layer can be tuned from paramagnetic to ferromagnetic, depending on the Eu metal coverage ($d_{Eu} = 1$ ML and 2 ML, respectively), and show, using angle-resolved photoemission spectroscopy (ARPES), that the integrity of the 2DES is preserved in both cases, thus providing an ideal knob for tuning the spin-transport properties of the 2DES. Our approach relies on recent results demonstrating that the evaporation of an amorphous ultrathin layer of Al metal on top of an oxide surface generates a homogeneous 2DES [24]. As the redox reaction between oxides and elementary metals with a large heat of formation of the corresponding metal oxide is a general phenomenon [25], 2DESs can be created in various oxides, e.g., $SrTiO_3$, TiO_2, and $BaTiO_3$ [24]. In the present study, we advance this exciting possibility towards simultaneously creating a 2DES and forming a *functional* metal oxide overlayer—i.e., in a macroscopic ferromagnetic ground state—by choosing a suitable elementary metal (Eu). Our experiments demonstrate how to elegantly link the simplicity and universality of an interfacial redox reaction to obtain increased functionalities by engineering *just one* active oxide overlayer that can enhance, modify, and allow controlling the properties of the subjacent so-created confined electron system.

Methods. The preparation of ultrathin EuO films by oxide molecular beam epitaxy (MBE) poses several experimental challenges [26–35]. The oxygen partial pressure, the substrate temperature, and the rate of impinging Eu-metal atoms must be carefully controlled. However, only the stoichiometric compound yields the desired simultaneous occurrence of magnetic and semiconducting behaviors. In this paper a

*mart.mueller@fz-juelich.de

†andres.santander@csnsm.in2p3.fr

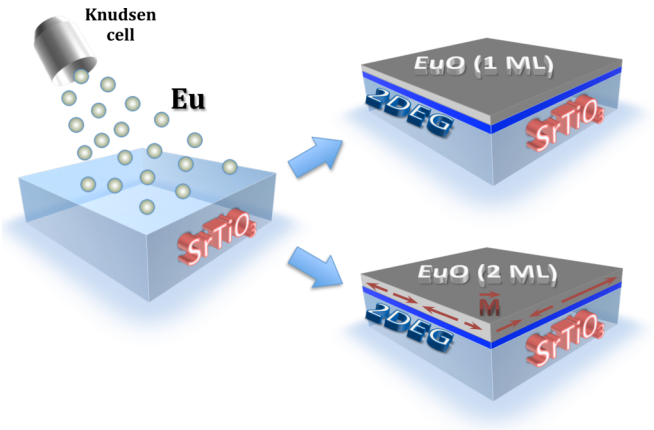

FIG. 1. Schematics of the experiment. Pure Eu metal (gray balls), evaporated from a Knudsen cell, reacts with the $SrTiO_3$ surface, forming stoichiometric insulating EuO (gray). The redox reaction locally reduces the $SrTiO_3$ around its surface, creating a 2DEG (blue). The capping layer can be tuned from paramagnetic, for 1 ML of EuO, to ferromagnetic, for 2 ML of EuO, where magnetic domains with in-plane magnetization **M** are represented by the red arrows.

method to synthesize ultrathin EuO is demonstrated and put into practice, i.e., a controlled interfacial redox reaction with oxygen provided by the substrate material *only*.

The undoped TiO_2-terminated $SrTiO_3$ samples are prepared using a well established technique [36]. Atomic force microscopy images show a flat surface with steps of unit cell height and a roughness within one terrace of typically 150 pm and a c-direction miscut angle $<0.1°$. The samples are then annealed in vacuum to 500 °C for 0.5 h in a MBE chamber at a base pressure of 1.3×10^{-10} mbar prior to Eu evaporation and photoemission experiments. The cleanliness and crystallinity of the so-obtained surfaces are checked by *in situ* x-ray photoemission spectroscopy (XPS). Pure Eu metal is then evaporated at 480 °C at a rate of 0.3 Å min^{-1} using a low temperature Knudsen cell, while the $SrTiO_3$ substrate is kept at room temperature. The deposition rate of Eu metal is monitored by a calibrated quartz microbalance.

The redox-created oxidation state of the Eu on the $SrTiO_3$ surface is analyzed using XPS with Al K_α radiation from a SPECS x-ray anode and a PHOIBOS-100 hemispherical energy analyzer at FZ Jülich. The Eu $3d$ and Ti $2p$ core levels are analyzed to quantify the oxidation state of the deposited Eu metal and to observe the redox process with the substrate surface. Before the *ex situ* magnetization measurements, realized with a Quantum Design MPMS SQUID magnetometer, the EuO/$SrTiO_3$ samples are further capped with 15 nm of e-beam evaporated MgO to avoid additional oxidation. A hysteresis loop of $H = \pm 1500$ Oe at $T = 5$ K is performed, while temperature dependence is recorded with an aligning field of $H = 500$ Oe for $T = 5$ to 150 K. All magnetization data was measured in-plane.

The ARPES measurements are conducted at the CASSIOPEE beamline of synchrotron SOLEIL. The beamline is equipped with an MBE chamber allowing the *in situ* preparation of the $SrTiO_3$ surfaces and evaporation of the pure Eu metal using the same above-specified conditions.

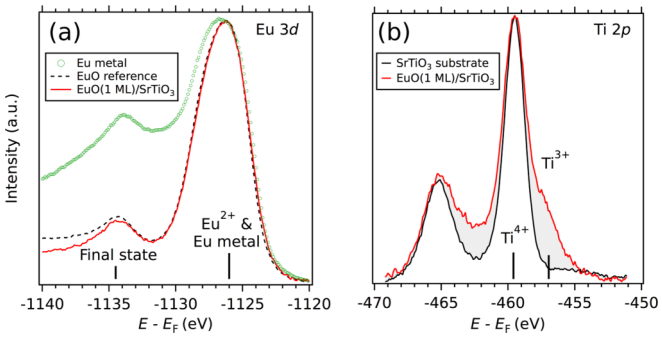

FIG. 2. XPS data of (a) the Eu $3d_{5/2}$ peak and (b) the Ti $2p$ core level. Both (a) and (b) illustrate the interfacial redox process after evaporation of pure Eu metal on the surface of $SrTiO_3$: Oxygen provided from the substrate forms 1 ML of stoichiometric EuO, while the Ti of the substrate is reduced to Ti^{3+}.

We furthermore checked that a surface cleaning using a much faster annealing (about one minute) creates a negligible amount of bulk oxygen vacancies. Eu evaporated hereafter then results in an identical 2DES, in line with previous reports showing that the electronic structure of the 2DES at the surface of $SrTiO_3$ is independent of the material's bulk doping [15]. We used linearly polarized photons at energies of 47 eV and 90 eV, which provide the best cross section for ARPES spectra on $SrTiO_3$ [15,24] and a hemispherical electron analyzer with vertical slits. The angular and energy resolutions were 0.1° and 8 meV. The mean diameter of the incident photon beam was smaller than 100 μm. The samples were measured at $T = 8$ K. The results were reproduced on two samples. All through this paper, we note $\langle hkl \rangle$ the directions in reciprocal space. The indices h, k, and l correspond to the reciprocal lattice vectors of the cubic unit cell of $SrTiO_3$.

Results. To show that ultrathin stoichiometric EuO can be grown without supplying additional oxygen, the films are analyzed using XPS. Figure 2(a) shows the Eu $3d_{5/2}$ core level. The chemistry of the film can be determined by comparison to reference spectra of Eu metal, Eu^{2+}, and Eu^{3+}. The dashed line represents stoichiometric EuO. In accordance with previous studies of the Eu $3d$ core level, the Eu^{2+} valence is located at an energy of -1125 eV [28,33,37]. The peak is accompanied by a well known satellite at higher binding energy, which is part of the multiplet of the $3d^9\,4f^7$ final state [37]. The red line shows the spectrum of a $SrTiO_3$ sample with 4Å of Eu metal deposited on top of it. The amount of Eu metal corresponds to a thickness of ≈1 ML of EuO. We find that the XPS spectra of our Eu-capped $SrTiO_3$ samples is indistinguishable from stoichiometric EuO reference data. Features related to Eu metal or Eu^{3+} are absent. Analogous results are found (not shown) in the case of a deposited Eu-metal layer of 8 Å. This demonstrates that, in the ultrahigh vacuum conditions used here, the Eu metal is oxidized into EuO at the surface of $SrTiO_3$.

The concomitant substrate reduction is evidenced by the analysis of the Ti $2p$ core level, shown in Fig. 2(b). For stoichiometric $SrTiO_3$ a pure Ti^{4+} valence is observed. Upon deposition of nominally 1 ML of EuO, the XPS spectrum shows an additional component at the binding energy of Ti^{3+}, indicating that the $SrTiO_3$ is indeed reduced.

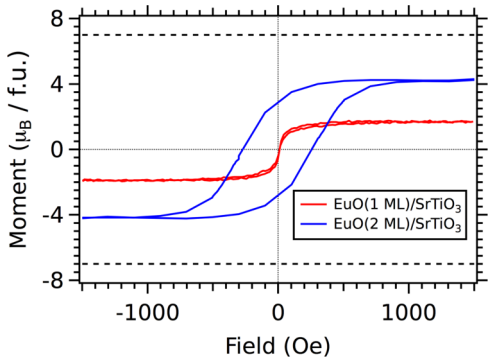

FIG. 3. In-plane magnetization curves measured at $T = 5$ K, obtained with a Quantum Design MPMS SQUID magnetometer, contrasting the paramagnetic behavior of 1 ML EuO and the low-dimensional ferromagnetic behavior of 2 ML EuO formed after evaporating pure Eu metal on TiO_2 terminated $SrTiO_3$. The horizontal dashed lines show the expected saturation magnetization at $T = 0$ K for EuO [26,38].

The unique properties of the obtained capping EuO layer, and their tuning with layer thickness, are presented in Fig. 3. The measured (not shown) ferromagnetic transition temperature of the 2 ML EuO film was $T \approx 60$ K. At $T = 5$ K, the magnetization versus field $M(H)$ curve of 1 ML of EuO (red curve) shows a paramagnetic behavior. In this case, the effective coordination number of Eu atoms is lower compared to the coordination number in bulk EuO, and thus exchange interactions are weakened [26]. However, at the same temperature, the 2 ML EuO overlayer is ferromagnetic (blue curve) with a saturation magnetization of $M_S = 4\ \mu_B$ per formula unit (f.u.). The measured saturated magnetic moment for 2 ML of EuO capping is close to the corresponding theoretical values for EuO at $T = 0$ K, represented by the horizontal dashed lines [26–28,38]. Now the underlying 2DES (see next) is interfaced with a magnetic material, which may ultimately enable a control of the spin degrees of freedom in this system.

The formation of oxygen vacancies near the $SrTiO_3$ surface, induced by the redox reaction with the Eu evaporated on top of it, results in a local electron doping of the substrate and the creation of a 2DES, in analogy with the 2DESs formed by oxygen vacancies at the UV-irradiated surface or Al-capped interface of $SrTiO_3$ or other oxides [15–18,21,24]. This is directly demonstrated by the ARPES data shown in Fig. 4. Figures 4(a) and 4(b) show the circular Fermi surfaces around Γ_{102} of the two $3d_{xy}$ subbands at the interfaces between 1 ML and 2 ML EuO films on $SrTiO_3$, respectively. Figures 4(c) and 4(d) present the corresponding energy-momentum ARPES intensity maps along the $k_{\langle 010\rangle}$ direction at $k_{\langle 100\rangle} = 2\pi/a$ ($a = 3.905$ Å is the lattice parameter of $SrTiO_3$). These correspond to the two Ti $3d_{xy}$ light subbands previously reported for the 2DES in $SrTiO_3$ [15,16,24]. For the 2DES at the EuO(1ML)/$SrTiO_3$ interface, the band bottoms ($E_0 \approx -200$ meV and -90 meV for the outer and inner subbands, respectively), Fermi momenta ($k_F \approx 0.19$ Å^{-1} and 0.12 Å^{-1}), effective masses ($m^*/m_e = 0.7 \pm 0.05$ for both subbands, estimated from a parabolic approximation to the band dispersions, where m_e is the bare electron mass), and the observation of a kink at $E \approx -30$ meV below E_F, ascribed

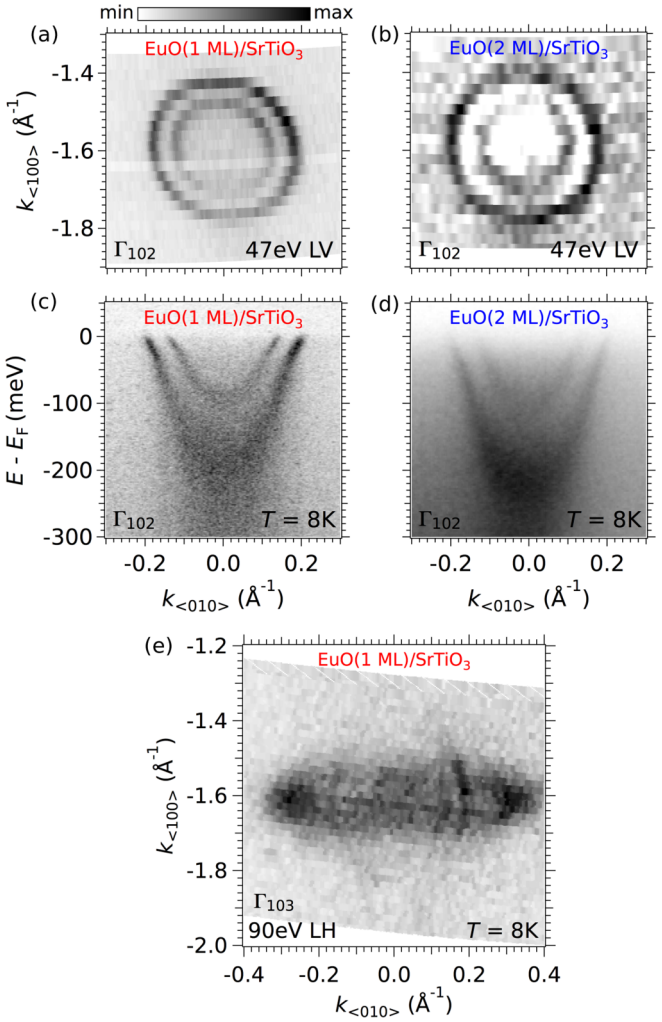

FIG. 4. ARPES data of the EuO/$SrTiO_3$ interface. (a), (b) Fermi surfaces taken around the Γ_{102} point of $SrTiO_3$ for nominally 1 ML (raw data) and 2 ML (negative values of second derivatives) EuO coverage, respectively, using 47 eV photons with linear vertical (LV) light polarization. These photon energy and polarization enhance the photoemission intensity of the $3d_{xy}$ circular Fermi surfaces. (c), (d) Corresponding dispersion of the two Ti $3d_{xy}$ light subbands. (e) Fermi surfaces taken around the Γ_{103} point of $SrTiO_3$ for 1 ML EuO coverage using 90 eV photons with linear horizontal (LH) light polarization. These photon energy and polarization enhance the photoemission intensity of one of the two orthogonal $3d_{xz/yz}$ ellipsoidal Fermi surfaces. As with our previous results on Al-capped $SrTiO_3$ [24], we crosschecked that for both 1 ML and 2 ML EuO the 2DEG forms instantaneously after the Eu deposition, and its carrier density is independent of the dose of UV light used to measure the ARPES data. In other words, the 2DEG is entirely due to the oxidation of the capping layer.

to a band renormalization due to electron-phonon interaction, are all in agreement with previous reports [15,16,24,39,40]. As shown in Fig. 4(e), the ellipsoidal Fermi surfaces, associated with the Ti $3d_{xz/yz}$ heavy subbands, are also observed using horizontal light polarization. From the total area A_F enclosed by *all* the Fermi surfaces, the density of carriers of the 2DES at the EuO/$SrTiO_3$ interfaces is $n_{2D} = A_F/(2\pi^2) \approx 2.0 \times 10^{14}$ cm^{-2}, which is comparable to the density of states

of the 2DES at the bare $SrTiO_3$ surface [15,24]. The thickness of the 2DES can be directly inferred from the number of subbands, their band bottoms and energy separations [15]. Thus, as the electronic structure of the 2DES at the EuO(1 ML)/$SrTiO_3$ interface is essentially the same as the one observed at the bare surface of $SrTiO_3$ [15], or at the Al-capped surface of $SrTiO_3$ [24], we conclude that its thickness is also the same, namely about 4–5 unit cells.

ARPES measurements are performed under zero external magnetic field, to guarantee conservation of the photoemitted electron momentum. Thus, while magnetizing the capping EuO film is not feasible for these measurements, it is nevertheless instructive to compare the ARPES data between the 1 ML and 2 ML EuO films, Figs. 4(a) and 4(c) and Figs. 4(b) and 4(d), respectively. Note that, while the Fermi momenta of the 2DESs in both systems are essentially identical, one observes a small but distinct difference in their bandwidths and band splittings. Specifically, in the case of the 2 ML EuO film, the bottoms of the Ti $3d_{xy}$ light subbands are at about -230 meV and -100 meV, with a concomitant band splitting ($\approx$130 meV) slightly larger than the one in the 1 ML EuO film ($\approx$100 meV). Additionally, both the Fermi edge at $E = 0$ and the kink at $E \approx -30$ meV appear much less pronounced in the 2DES at the EuO(2 ML)/$SrTiO_3$ interface. The possible link between such differences in electronic structure, and the ferromagnetism (with or without domains) in the 2 ML EuO film, should be further explored in future works. On the other hand, an important conclusion at this point is that the onset of ferromagnetism in the zero-field-cooled 2 ML EuO films, with the concomitant formation of randomly oriented ferromagnetic domains (as schematized in Fig. 1), still preserves the integrity of the underlying 2DES. Together with the magnetization data from Fig. 3, our results open the very exciting perspective of enabling the continuous tuning, under external applied field, of the spin transport properties in oxide-based 2DES.

Conclusions. In summary, we demonstrated that the deposition in vacuum, at room temperature, of Eu metal on $SrTiO_3$ results in the simultaneous creation of a 2DES in the oxide substrate and a capping EuO layer that can be tuned from paramagnetic (1 ML thickness) to ferromagnetic (2 ML). These results open new perspectives for investigating the interaction of the magnetic and electronic properties of the 2DES in $SrTiO_3$. More generally, these results lay a new ground for the simple and versatile design of all-oxide devices in which the functionalities of the constituting elements, and their mutual coupling, can be obtained from controlled physicochemical reactions and vacancy engineering at their interfaces.

Acknowledgments. We thank O. Petracic and the Jülich Centre for Neutron science for providing measurement time at the SQUID magnetometer. Work at CSNSM was supported by public grants from the French National Research Agency (ANR), project LACUNES No ANR-13-BS04-0006-01, and the "Laboratoire d'Excellence Physique Atomes Lumière Matière" (LabEx PALM projects ELECTROX and 2DEG2USE) overseen by the ANR as part of the "Investissements d'Avenir" program (reference: ANR-10-LABX-0039). M.M. acknowledges financial support from HGF under Contract No. VH-NG-811. T.C.R. acknowledges funding from the RTRA–Triangle de la Physique (project PEGASOS). A.F.S.-S. thanks support from the Institut Universitaire de France.

P.L. and T.C.R. contributed equally to this work.

[1] A. Ohtomo and H. Y. Hwang, Nature (London) **427**, 423 (2004).
[2] S. Thiel, G. Hammerl, A. Schmehl, C. W. Schneider, and J. Mannhart, Science **313**, 1942 (2006).
[3] N. Reyren, S. Thiel, A. D. Caviglia, L. Fitting Kourkoutis, G. Hammerl, C. Richter, C. W. Schneider, T. Kopp, A.-S. Rüetschi, D. Jaccard, M. Gabay, D. A. Muller, J.-M. Triscone, and J. Mannhart, Science **317**, 1196 (2007).
[4] K. Ueno, S. Nakamura, H. Shimotani, A. Ohtomo, N. Kimura, T. Nojima, H. Aoki, Y. Iwasa, and M. Kawasaki, Nat. Mater. **7**, 855 (2008).
[5] H. Nakamura, H. Tomita, H. Akimoto, R. Matsumura, I. H. Inoue, T. Hasegawa, K. Kono, Y. Tokura, and H. Takagi, J. Phys. Soc. Jpn. **78**, 083713 (2009).
[6] A. Brinkman, M. Huijben, M. van Zalk, J. Huijben, U. Zeitler, J. C. Maan, W. G. van der Wiel, G. Rijnders, D. H. A. Blank, and H. Hilgenkamp, Nat. Mater. **6**, 493 (2007).
[7] A. D. Caviglia, S. Gariglio, N. Reyren, D. Jaccard, T. Schneider, M. Gabay, S. Thiel, G. Hammerl, J. Mannhart, and J.-M. Triscone, Nature (London) **456**, 624 (2008).
[8] A. D. Caviglia, M. Gabay, S. Gariglio, N. Reyren, C. Cancellieri, and J. M. Triscone, Phys. Rev. Lett. **104**, 126803 (2010).
[9] A. Joshua, J. Ruhman, S. Pecker, E. Altman, and S. Ilani, Proc. Natl. Acad. Sci. **110**, 9633 (2013).
[10] T. D. Ngo, J.-W. Chang, K. Lee, S. Han, J. S. Lee, Y. H. Kim, M.-H. Jung, Y.-J. Doh, M.-S. Choi, J. Song, and J. Kim, Nat. Commun. **6**, 8035 (2015).
[11] E. Lesne, Y. Fu, S. Oyarzun, J. C. Rojas-Sánchez, D. C. Vaz, H. Naganuma, G. Sicoli, J.-P. Attané, M. Jamet, E. Jacquet, J.-M. George, A. Barthélémy, H. Jaffrès, A. Fert, M. Bibes, and L. Vila, Nat. Mater. **15**, 1261 (2016).
[12] Q. Song, H. Zhang, T. Su, W. Yuan, Y. Chen, W. Xing, J. Shi, J.-R. Sun, and W. Han, Sci. Adv. **3**, e1602312 (2017).
[13] D. Stornaiuolo, C. Cantoni, G. M. De Luca, R. Di Capua, E. Di Gennaro, G. Ghiringhelli, B. Jouault, D. Marrè, D. Massarotti, F. Miletto Granozio, I. Pallecchi, C. Piamonteze, S. Rusponi, F. Tafuri, and M. Salluzzo, Nat. Mater. **15**, 278 (2016).
[14] V. T. Tra, J.-W. Chen, P.-C. Huang, B.-C. Huang, Y. Cao, C.-H. Yeh, H.-J. Liu, E. A. Eliseev, A. N. Morozovska, J.-Y. Lin, Y.-C. Chen, M.-W. Chu, P.-W. Chiu, Y.-P. Chiu, L.-Q. Chen, C.-L. Wu, and Y.-H. Chu, Adv. Mater. **25**, 3357 (2013).
[15] A. F. Santander-Syro, O. Copie, T. Kondo, F. Fortuna, S. Pailhes, R. Weht, X. G. Qiu, F. Bertran, A. Nicolaou, A. Taleb-Ibrahimi, P. Le Fèvre, G. Herranz, M. Bibes, N. Reyren, Y. Apertet, P. Lecoeur, A. Barthélémy, and M. J. Rozenberg, Nature (London) **469**, 189 (2011).
[16] W. Meevasana, P. D. C. King, R. H. He, S.-K. Mo, M. Hashimoto, A. Tamai, P. Songsiriritthigul, F. Baumberger, and Z.-X. Shen, Nat. Mater. **10**, 114 (2011).
[17] A. F. Santander-Syro, C. Bareille, F. Fortuna, O. Copie, M. Gabay, F. Bertran, A. Taleb-Ibrahimi, P. Le Fèvre, G. Herranz, N. Reyren, M. Bibes, A. Barthélémy, P. Lecoeur, J. Guevara, and M. J. Rozenberg, Phys. Rev. B **86**, 121107 (2012).

[18] C. Bareille, F. Fortuna, T. C. Rödel, F. Bertran, M. Gabay, O. Hijano Cubelos, A. Taleb-Ibrahimi, P. Le Fèvre, M. Bibes, A. Barthélémy, T. Maroutian, P. Lecoeur, M. J. Rozenberg, and A. F. Santander-Syro, Sci. Rep. **4**, 3586 (2014).

[19] T. C. Rödel, C. Bareille, F. Fortuna, C. Baumier, F. Bertran, P. Le Fèvre, M. Gabay, O. Hijano Cubelos, M. J. Rozenberg, T. Maroutian, P. Lecoeur, and A. F. Santander-Syro, Phys. Rev. Appl. **1**, 051002 (2014).

[20] A. F. Santander-Syro, F. Fortuna, C. Bareille, T. C. Rödel, G. Landolt, N. C. Plumb, J. H. Dil, and M. Radović, Nat. Mater. **13**, 1085 (2014).

[21] T. C. Rödel, F. Fortuna, F. Bertran, M. Gabay, M. J. Rozenberg, A. F. Santander-Syro, and P. Le Fèvre, Phys. Rev. B **92**, 041106(R) (2015).

[22] E. Frantzeskakis, T. C. Rödel, F. Fortuna, and A. F. Santander-Syro, J. Electron Spectrosc. Relat. Phenom. **219**, 16 (2017).

[23] T. Taniuchi, Y. Motoyui, K. Morozumi, T. C. Rödel, F. Fortuna, A. F. Santander-Syro, and S. Shin, Nat. Commun. **7**, 11781 (2016).

[24] T. C. Rödel, F. Fortuna, S. Sengupta, E. Frantzeskakis, P. Le Fèvre, F. Bertran, B. Mercey, S. Matzen, G. Agnus, T. Maroutian, P. Lecoeur, and A. F. Santander-Syro, Adv. Mater. **28**, 1976 (2016).

[25] C. T. Campbell, J. Chem. Soc. Faraday Trans. **92**, 1435 (1996).

[26] M. Müller, G.-X. Miao, and J. S. Moodera, J. Appl. Phys. **105**, 07C917 (2009).

[27] C. Caspers, A. Gloskovskij, W. Drube, C. M. Schneider, and M. Müller, Phys. Rev. B **88**, 245302 (2013).

[28] T. Gerber, P. Lömker, B. Zijlstra, C. Besson, D. N. Mueller, W. Zander, J. Schubert, M. Gorgoi, and M. Müller, J. Mater. Chem. C **4**, 1813 (2016).

[29] P. G. Steeneken, Ph.D. thesis, Rijksuniversiteit Groningen, Groningen, Netherlands, 2002.

[30] R. W. Ulbricht, A. Schmehl, T. Heeg, J. Schubert, and D. G. Schlom, Appl. Phys. Lett. **93**, 102105 (2008).

[31] R. Sutarto, S. G. Altendorf, B. Coloru, M. Moretti Sala, T. Haupricht, C. F. Chang, Z. Hu, C. Schüßler-Langeheine, N. Hollmann, H. Kierspel, H. H. Hsieh, H. J. Lin, C. T. Chen, and L. H. Tjeng, Phys. Rev. B **79**, 205318 (2009).

[32] D. F. Förster, J. Klinkhammer, C. Busse, S. G. Altendorf, T. Michely, Z. Hu, Y.-Y. Chin, L. H. Tjeng, J. Coraux, and D. Bourgault, Phys. Rev. B **83**, 045424 (2011).

[33] C. Caspers, M. Müller, A. X. Gray, A. M. Kaiser, A. Gloskovskii, C. S. Fadley, W. Drube, and C. M. Schneider, Phys. Rev. B **84**, 205217 (2011).

[34] C. Caspers, A. Gloskovskii, M. Gorgoi, C. Besson, M. Luysberg, K. Rushchanskii, M. Lezaic, C. S. Fadley, W. Drube, and M. Müller, Sci. Rep. **6**, 22912 (2016).

[35] G. Prinz, T. Gerber, A. Lorke, and M. Müller, Appl. Phys. Lett. **109**, 202401 (2016).

[36] G. Koster, B. L. Kropman, G. J. H. M. Rijnders, D. H. A. Blank, and H. Rogalla, Appl. Phys. Lett. **73**, 2920 (1998).

[37] E.-J. Cho, S.-J. Oh, S. Imada, S. Suga, T. Suzuki, and T. Kasuya, Phys. Rev. B **51**, 10146 (1995).

[38] R. Schiller and W. Nolting, Phys. Rev. Lett. **86**, 3847 (2001).

[39] C. Chen, J. Avila, E. Frantzeskakis, A. Levy, and M. C. Asensio, Nat. Commun. **6**, 8585 (2015).

[40] Z. Wang, S. McKeown Walker, A. Tamai, Y. Wang, Z. Ristic, F. Y. Bruno, A. de la Torre, S. Riccò, N. C. Plumb, M. Shi, P. Hlawenka, J. Sánchez-Barriga, A. Varykhalov, T. K. Kim, M. Hoesch, P. D. C. King, W. Meevasana, U. Diebold, J. Mesot, B. Moritz, T. P. Devereaux, M. Radović, and F. Baumberger, Nat. Mater. **15**, 835 (2016).